Reaction Pathways and Site Requirements for the Activation and Chemical Conversion of Methane on Ru−Based Catalysts

Junmei Wei and Enrique Iglesia*

Department of Chemical Engineering, University of California at Berkeley, Berkeley, California 94720

Received: June 24, 2003; In Final Form: September 29, 2003

Kinetic and isotopic tracer and exchange measurements were used to determine the identity and reversibility of elementary steps required for CH_4 reforming reactions on Ru-based catalyst. These studies provide a simple mechanistic picture and a unifying kinetic treatment for CH_4/CO_2 and CH_4/H_2O reforming reactions and CH_4 decomposition. Forward kinetic rates were measured from net rates by correcting for the approach to equilibrium, after ruling out transport artifacts using pellet and bed dilution tests. The kinetic processes involved are exclusively limited by C−H bond activation, and CH_4 reaction rates are unaffected by the identity or the concentration of co-reactants (H_2O, CO_2). Similar normal kinetic isotopic effects ($k_{C-H}/k_{C-D} = 1.40-1.51$) were measured for CO_2 reforming, H_2O reforming, and CH_4 decomposition, consistent with kinetically relevant C−H bond activation steps. The ratio of CH_4/CD_4 cross-exchange to methane chemical conversion rates during the reaction of CO_2 reforming with CH_4-CD_4 mixtures was 0.05, suggesting that steps involving C−H bond activation are essentially irreversible. Binomial D-atom distributions in dihydrogen and water were obtained during reactions of $CH_4/CO_2/D_2$ mixtures, and their D-contents were identical to those expected from complete equilibration between D_2 and H-atoms from reacted CH_4, indicating that H−OH and H−H recombination steps are quasi-equilibrated. Reactions of $^{12}CH_4/^{12}CO_2/^{13}CO$ mixtures gave identical ^{13}C contents in CO and CO_2, even far away from the CO_2 reforming equilibrium; thus, CO_2 activation is reversible and quasi-equilibrated during CO_2 reforming on Ru-based catalysts, as expected from the kinetic irrelevance of co-reactant activation steps. These conclusions suggest that water-gas shift reactions are also equilibrated, as confirmed by chemical analyses of reaction products. Forward CH_4 turnover rates increased with increasing Ru dispersion, but they were essentially unaffected by the identity of the support. This behavior reflects the higher reactivity of coordinatively unsaturated surface atoms, prevalent in small Ru clusters, for C−H bond activation reactions, as previously inferred from the effect of crystal orientation on CH_4 activation rates.

Introduction

CH_4 reactions with CO_2 or H_2O can be used to produce synthesis gas mixtures for ultimate conversion to desired fuels and chemicals. Fischer and Tropsch[1] first showed that group VIII metals (Ni, Ru, Rh, Pt, Pd, and Ir) catalyzed CO_2-CH_4 reactions to form these H_2-CO mixtures. Specifically, Ru clusters supported on Al_2O_3,[2−13] TiO_2,[2,14] MgO,[15,16] La_2O_3,[7−9] SiO_2,[12,17] NaY,[18] and carbon[2,19] effectively catalyze these reactions. The relevant elementary steps and the effects of metal dispersion and support on reaction rates have not been unequivocally established on supported Ru catalysts.

Bifunctional CO_2 reforming pathways on Ru/Al_2O_3 were proposed to involve CH_4 decomposition on Ru and CO_2 activation on OH groups in the Al_2O_3 support.[11] Matsui et al.[9] proposed a redox mechanism on Ru supported on La_2O_3, ZrO_2, and Y_2O_3, in which CH_4 forms $Ru-CH_x$ species and CO_2 dissociates to form CO and chemisorbed oxygen atoms; $Ru-CH_x$ then reacts with chemisorbed oxygen atoms to form CO and Ru. Mark and Maier[10] proposed rate-determining CH_4 decomposition steps to form chemisorbed carbon and H_2, and the reaction of carbon with CO_2 in a fast process; this proposal led to a rate equation consistent with kinetic data:

$$r = \frac{k(P_{CH_4} - (P_{H_2}{}^2 P_{CO}{}^2/\alpha P_{CO_2}))}{1+(P_{CO}{}^2/\beta P_{CO_2})} \quad (1)$$

Studies of the stoichiometric activation of CO_2 and CH_4 on Ru/Al_2O_3 led to a proposal that CH_4 dissociation is aided by chemisorbed oxygen formed via CO_2 dissociation; the latter was in turn promoted by chemisorbed H-atoms formed in C−H bond activation.[3] CO_2 reforming turnover rates on Ru/TiO_2, Ru/C, and Ru/Al_2O_3 were influenced by conversion, because reverse steps contributed to measured rates as reactions approached equilibrium.[2] After corrections for reverse reactions, forward rates were accurately described by a simple rate equation:

$$r_f = k_f P_{CH_4}{}^a P_{CO_2}{}^b \quad (2)$$

where a and b are given by $0.52(\pm 0.36)$ and $0.21(\pm 0.40)$, respectively. This expression was shown to be consistent with a sequence involving slow and reversible CH_4 dissociation to form CH_x species and irreversible slow decomposition of CH_xO species to form CO and hydrogen, but these conclusions remained speculative because of large uncertainties in reported reaction orders.

Rostrup-Nielsen and Hansen[16] reported the only parallel study of CO_2 and H_2O reforming reactions on Ru catalysts. They proposed that CO_2 and H_2O reforming mechanisms are similar

* Author to whom correspondence should be addressed. Tel: (510) 642-9673. Fax: (510) 642-4778. E-mail: iglesia@cchem.berkeley.edu.

10.1021/jp030783l CCC: $27.50
Published on Web 04/29/2004

on Ru/MgO, but found significantly higher reaction rates for H_2O reforming (80 kPa H_2O, 20 kPa CH_4) (8.9 mol site^{-1} s^{-1}) than for CO_2 reforming (80 kPa CO_2, 20 kPa CH_4) (2.9 mol site^{-1} s^{-1}) at 823 K. These authors proposed that the replacement of H_2O co-reactants with CO_2 introduced a kinetic bottleneck associated with CO_2 activation, which became the rate-determining step in CO_2 reforming reactions

Several studies on model metal surfaces have concluded that C−H bond activation is probably the kinetically relevant step in CH_4 conversion reactions, but these studies have measured only rates of stoichiometric CH_4 decomposition reactions, typically at temperatures much lower than those required to overcome kinetic and thermodynamic hurdles during CH_4 reforming catalysis.[20(and refs therein)] For these systems and reactions, C−H bond dissociation occurs more rapidly on step and kink sites than on terrace sites, apparently because of the higher reactivity of coordinatively unsaturated surface metal atoms.[22−24] Stoichiometric activation of CH_4 appears to depend sensitively on surface structure; this structure sensitivity, by the definition of Boudart,[21] should lead to strong effects of metal cluster size on catalytic turnover rates. Yet, we have not found systematic studies of dispersion effects on CH_4 reactions catalyzed by Ru or of the effects of Ru surface structure on catalytic reforming reactions.

The supports used to disperse Ru crystallites often influence CO_2 reforming rates, but concurrent effects of supports on Ru dispersion, on transport artifacts, or on approach to equilibrium are seldom independently considered. Matsui[9] found that CH_4 conversions in CO_2 reforming were higher on Ru/ZrO_2 and Ru/La_2O_3 than on Ru/Al_2O_3, and proposed, without direct evidence, that such effects arose from the different reactivities of the various supports in CO_2 activation. Ferreira-Aparicio et al.[11] suggested that OH groups on supports catalyzed rate-determining CO_2 activation steps. Bradford and Vannice[2] found higher turnover rates when Ru was dispersed on TiO_2 than on Al_2O_3 or carbon, even though Ru dispersions (from H_2 chemisorption) were lower on TiO_2 (51%) supports than on Al_2O_3 (78%) or carbon (100%) supports. This study provided infrared evidence for the decoration of Ru crystallites with TiO_x species during catalyst reduction and proposed that such sites exhibit unique catalytic activity because of the resulting intimate metal−support contacts. The nature of these interactions, their specific role in kinetically relevant steps, and even the survival of these decoration effects in contact with CO_2 and H_2O at high temperatures remain unclear.

Here, we probe the identity and reversibility of elementary steps required for H_2O and CO_2 reforming of CH_4 on supported Ru catalysts. We provide evidence for a catalytic sequence that rigorously combines the kinetics and pathways for water-gas shift, CH_4 decomposition, and CO_2 and H_2O reforming reactions. Kinetic and isotopic experiments confirmed this sequence and established the sole kinetic relevance of C−H bond activation and the essentially uncovered nature of Ru surfaces during steady-state catalysis. Reaction rates were measured in the absence of transport artifacts and rigorously corrected for the approach to equilibrium of reforming reactions. Similar rate constants determined for C−H bond activation in H_2O reforming, CO_2 reforming, and CH_4 decomposition reactions are compared on samples with varying Ru dispersion on Al_2O_3 and ZrO_2 supports. Turnover rates were strongly influenced by Ru dispersion but essentially insensitive to the support used and to the identity or concentration of the co-reactant, consistent with CH_4 activation rate-determining steps and with the kinetic irrelevance of CO_2 and H_2O activation. These conclusions resemble those reached in our recent studies of CH_4 reforming and decomposition reactions on Rh,[25] Pt,[26] Ir,[27] and Ni[28] catalysts, the evidence for which is presented elsewhere.

Experimental Methods

Ru/Al_2O_3 with 1.6 and 3.2 wt % Ru and Ru/ZrO_2 with 3.2 wt % Ru were prepared by incipient wetness impregnation of Al_2O_3 or ZrO_2 with an aqueous solution of $Ru(NO)(NH_3)_3$ (Alfa, CAS#34513-98-9). Impregnated samples were dried at 393 K in ambient air and treated in flowing dry air (Airgas, UHP, 1.2 cm^3/g-s) by increasing the temperature to 873 K at 0.167 K s^{-1} and holding at 873 K for 5 h. Samples were then treated in H_2 (Airgas, UHP, 50 cm^3/g-s) by heating to 873 K at 0.167 K s^{-1} and holding at 873 K for 2 h. The 3.2 wt % Ru/Al_2O_3 sample was also treated in H_2 (Airgas, UHP, 50 cm^3/g-s) by increasing the temperature to 1023 K at 0.167 K s^{-1} and holding at 1023 K for 2 h in order to vary the size of Ru clusters. Al_2O_3 (160 m^2/g) was prepared by treating $Al(OH)_3$ (Aldrich, 21645-51-2) in flowing dry air (Airgas, UHP, 1.2 cm^3/g-s) while increasing the temperature to 923 K at 0.167 K s^{-1} and holding at 923 K for 5 h, a procedure that leads to γ-Al_2O_3.[29] ZrO_2 (45 m^2/g) was prepared by hydrolysis of a 0.5 M aqueous solution of $ZrOCl_2 \cdot 8H_2O$ (Aldrich, >98 wt %) at a constant pH of 10, maintained by addition of controlled amounts of a 14.8 M NH_4OH solution.[30] The precipitates were immediately filtered and washed repeatedly by redispersing it in a warm NH_4OH solution (pH 10, ~333 K) to remove residual Cl ions, until no Cl ions were detected by a $AgNO_3$ test (Cl^- < 10 ppm). The samples were then dried at 393 K overnight in ambient air and treated in flowing dry air (Airgas, UHP, 1.2 cm^3/g-s) by heating to 923 K at 0.167 K s^{-1} and holding at 923 K for 5 h. X-ray diffraction showed the predominant presence of monoclinic ZrO_2.

Ru dispersion was measured by volumetric H_2 chemisorption at 373 K[31] using a Quantasorb chemisorption analyzer (Quantachrome Corp.). Catalysts were reduced in H_2 at 873 K for 2 h, and then evacuated at 873 K for 0.5 h. After cooling to 373 K, a H_2 chemisorption isotherm was measured between 3 and 50 kPa. A backsorption isotherm was measured by repeating this procedure after evacuating samples at 373 K for 0.5 h. Both isotherms were extrapolated to zero H_2 pressure and their difference used as a measure of the uptake of strongly chemisorbed hydrogen. Ru dispersions were calculated by assuming that one hydrogen atom chemisorbed on each surface Ru;[31] dispersion values are shown in Table 1 for each of the catalysts used in this study.

Catalytic rates were measured by placing samples (5 mg, 250−425 μm) within a quartz or steel tube (8 mm inner diameter) with a type K thermocouple enclosed within a sheath in contact with the catalyst bed. Samples were diluted with ground, acid-washed quartz powder (500 mg, 250−425 μm) to avoid temperature gradients. Transport artifacts were ruled out using pellet and bed dilution with the pure support without detectable changes in rates or selectivities, as shown in the Appendix. The effects of CH_4, H_2O, and CO_2 pressures on CH_4 reaction rates were measured at 823−1023 K and 0.1−0.5 MPa total pressure over a wide range of reactant concentrations. Reactant mixtures were prepared using 50% CH_4/Ar (Matheson) and 50% CO_2/Ar (Matheson) certified mixtures and He (Airgas, UHP) as balance. For H_2O reforming reactions, H_2O was introduced using a syringe pump (Cole-Parmer, 74900 series). All transfer lines after H_2O introduction

TABLE 1: Forward CH_4 Turnover Rate on Supported Ru Catalysts (873 K, 20 kPa CH_4, 20 kPa CO_2 or H_2O)

catalyst	reduction temperature (K)	Ru dispersion (%)	Forward CH_4 Turnover Rate (s^{-1}) CH_4-CO_2	CH_4-H_2O	CH_4 decomposition	reference
1.6 wt % Ru/γ-Al_2O_3	873	55.5	4.8	4.9		this study
3.2 wt % Ru/γ-Al_2O_3	873	44.2	3.1	3.3	3.1	this study
3.2 wt % Ru/γ-Al_2O_3	1023	33.1	2.7	2.6		this study
3.2 wt % Ru/ZrO_2	873	29.8	2.5	2.3	2.2	this study
1.6 wt % Ru/η-Al_2O_3		78.0	15.3[a]			2
4.8 wt % Ru/C		100	1.1[a]			2
1.0 wt % Ru/γ-Al_2O_3		5.5	1.2[a]			3
0.64 wt % Ru/γ-Al_2O_3		51.0	5.1[a]			12
1.0 wt % Ru/NaY		28.0	2.6[a]			18

[a] Net rates were corrected to forward rates by approach to equilibrium using eq 5, then extrapolated to our reaction conditions (873 K, 20 kPa CH_4) using $r = A \exp(-Ea/RT)\ P_{CH_4}$.

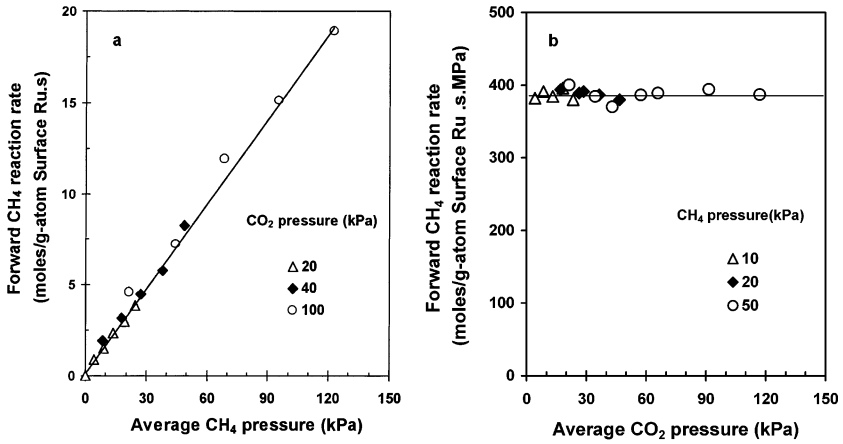

Figure 1. Effects of CH_4 (a) and CO_2 (b) partial pressure on forward CH_4 reaction rate for CO_2 reforming of CH_4 on 3.2 wt % Ru/Al_2O_3 reduced at 873 K (5 mg catalyst, 873 K, total flow rate 100 cm^3/min, balance He, average pressure is the average of inlet and outlet pressures of the reactor).

were kept above 373 K to avoid condensation. Reactant and product concentrations were measured with a Hewlett-Packard 6890 gas chromatograph using a Carboxen 1000 packed column (3.2 mm × 2 m) and thermal conductivity detection. Unless otherwise noted, catalysts were reduced at 873 K before CH_4 reforming reactions. No products were detected at 823−1023 K in empty reactors.

Ru/Al_2O_3 and Ru/ZrO_2 catalysts (20 mg, treated in H_2 at 873 K; 3.2 wt %) diluted with 500 mg quartz powder were used for CH_4 and CD_4 decomposition reactions at 873 K. Chemical compositions were measured by on-line mass spectrometry (Leybold Inficon, Transpector Series). Reactant mixtures with 20% CH_4/Ar or 20% CD_4/Ar were prepared using 50% CH_4/Ar (Matheson, certified mixture) or CD_4 (Isotec, chemical purity > 99.0%) with Ar (Airgas, UHP) as an inert internal standard used for accurate CH_4 conversion measurements. Initial CH_4 decomposition rates were used to estimate rate constants for CH_4 decomposition using the observed linear dependence of rates on CH_4 concentration.

Isotopic tracer studies were carried out on 3.2 wt % Ru/Al_2O_3 reduced at 873 K with a 44.2% Ru dispersion using a transient flow apparatus with short hydrodynamic delays (<5 s). Chemical and isotopic compositions were measured using on-line mass spectrometry (Leybold Inficon, Transpector Series). CD_4 (Isotec, chemical purity > 99.0%), D_2O (Isotec, chemical purity > 99.0%), and 5% D_2/Ar and ^{13}CO (Isotec, chemical purity > 99.0%) were used as reactants without further purification. Intensities at 15 and 17−20 amu were used to measure methane isotopomer concentrations. CH_4 and CD_4 standard fragmentation patterns were measured, and those for CHD_3, CH_2D_2, and CH_3D were calculated using reported methods.[32] Intensities at 18, 19, and 20 amu were used to determine water isotopomers and those at 28, 29, 44, and 45 amu to measure ^{12}CO, ^{13}CO, $^{12}CO_2$, and $^{13}CO_2$ concentrations, respectively. Detailed experimental conditions are shown together with the corresponding data in the Results section.

Carbon formation rates were measured during reforming reactions at 873 K using a tapered element quartz oscillating microbalance (Rupprecht & Patashnick, Series 1500). Catalyst treatment procedures and reaction conditions were similar to those used in kinetic measurements.

Results and Discussion

Kinetic Dependence of Reforming Rates on CH_4, CO_2, and H_2O Partial Pressures. The kinetic dependence of CH_4 reforming rates on CH_4, CO_2, and H_2O concentrations was measured on 3.2 wt % Ru/Al_2O_3 treated at 873 K in H_2 (44.2% Ru dispersion) at conditions leading to stable rates and undetectable carbon formation. Filament carbon formation was not detected in parallel microbalance experiments or by transmission electron microscopy analyses of catalyst samples after use.

Figure 1 shows the effects of CH_4 and CO_2 pressures on forward CH_4 turnover rate (r_f, normalized by the number of exposed surface Ru atoms) at 873 K and 100−500 kPa total pressure. Net rate measurements far from equilibrium require very low CH_4 conversions at low temperatures, because of unfavorable thermodynamics, and they become impractical at high temperatures, because very fast reaction rates lead to ubiquitous temperature and concentration gradients. Measured reaction rates were corrected for approach to equilibrium (η) using thermodynamic data[33] and prevalent pressures of reactants

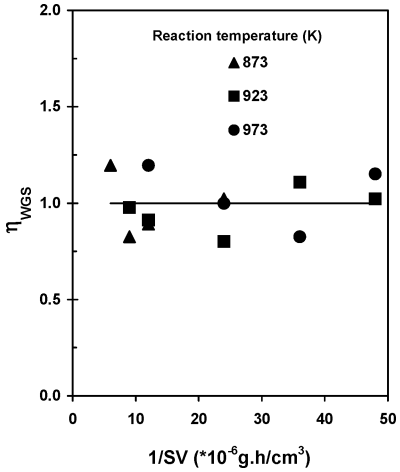

Figure 2. Extent of water-gas-shift equilibrium at different reaction temperatures as a function of space velocity on 3.2 wt % Ru/Al_2O_3 catalysts reduced at 873 K (44.2% Ru dispersion). (Reaction conditions: $CO_2/CH_4/Ar$ = 1:1:2, 100 kPa total pressure, $\eta_{WGS} = ([P_{CO}][P_{H_2O}])/([P_{H_2}][P_{CO_2}]K_{WGS})$).

and products to give forward rates for CH_4-CO_2 and CH_4-H_2O reactions:

$$\eta_1 = \frac{[P_{CO}]^2[P_{H_2}]^2}{[P_{CH_4}][P_{CO_2}]} \times \frac{1}{K_{EQ1}} \quad (3)$$

$$\eta_2 = \frac{[P_{CO}][P_{H_2}]^3}{[P_{CH_4}][P_{H_2O}]} \times \frac{1}{K_{EQ2}} \quad (4)$$

In these equations, $[P_j]$ is the average partial pressure of species j (in units of atm) in the reactor. Average pressures were used in order to correct for minor depletion of reactants along the catalyst bed. K_{EQ1} and K_{EQ2} are equilibrium constants for each reforming reaction.[33] The $(1 - \eta)$ values were larger than 0.8 for all catalytic measurements reported here. Net reaction rates (r_n) are used to obtain forward reaction rates using

$$r_n = (r_f - r_r) = r_f(1 - \eta) \quad (5)$$

where r_r is the reverse reaction rate.[34] This equation accurately described the observed effects of reactor residence time and CH_4 conversion level on reforming rates.

Forward CH_4-CO_2 reaction rates increased linearly with increasing CH_4 partial pressure (5−125 kPa) at 873 K and were independent of CO_2 partial pressure (5−125 kPa) (Figure 1(a,b)). Forward rates were also insensitive to CO, H_2, and H_2O pressures, whether these pressures were varied by adding these species to the inlet stream or by changing residence times and CH_4 conversions. Measured concentrations during CH_4 reforming corresponded to equilibrated water-gas-shift (WGS) reactions at all temperatures between 823 and 1023 K (Figure 2). CH_4-CO_2 reaction rates are simply described by a first-order dependence in CH_4 and a zero-order dependence in CO_2,

$$r_f = k_{CO_2} P_{CH_4} \quad (6)$$

Once reverse reaction rates are considered using eqs 3−5, this expression describes CO_2 reforming rates at all temperatures (823−1023 K).

More complex rate expressions reported in previous studies[3,10] may reflect transport artifacts or nonrigorous accounts of reverse reactions. Equation 6 is consistent with CH_4 activation on Ru surfaces as the sole kinetically relevant elementary step and with fast steps involving recombinative hydrogen desorption to form H_2 and reactions of CO_2 with CH_4-derived chemisorbed species to form CO. These fast steps maintain Ru surfaces essentially uncovered by reactive intermediates during CH_4-CO_2 reactions. Otherwise, higher CO_2 pressure would increase the rate of removal of adsorbed intermediates and lead to positive effects on CH_4 reforming rates. These data do not preclude the presence of completely unreactive residues during catalysis, an issue that we address below.

The kinetic irrelevance of carbon removal by co-reactants and the mechanistic equivalence of H_2O and CO_2 reforming reactions were confirmed by CH_4-H_2O reaction rates measured on 3.2 wt % Ru/Al_2O_3. These rates are shown together with those for CH_4-CO_2 reactions in Figure 3 as a function of CH_4 and co-reactant pressures. Forward CH_4-H_2O reaction rates are proportional to CH_4 partial pressures (5−25 kPa) and independent of H_2O partial pressure (5−25 kPa). As in CH_4-CO_2 reactions, rates are simply described by

$$r_f = k_{H_2O} P_{CH_4} \quad (7)$$

Rate constants for H_2O (k_{H_2O}) and CO_2 (k_{CO_2}) reforming are similar to each other at each reaction temperature (Figure 4) and show similar activation energies. The corresponding pre-exponential factors for these rate constants are shown in Table

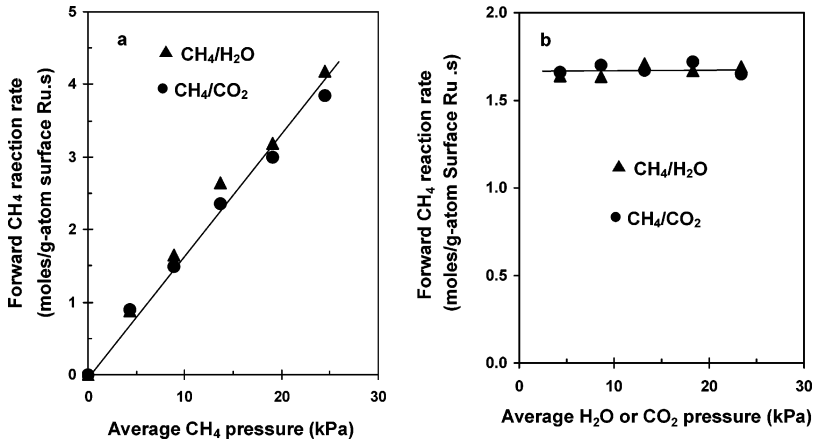

Figure 3. Effects of CH_4 (a) and CO_2 or H_2O (b) partial pressure on forward CH_4 reaction rate for CH_4-CO_2 and CH_4-H_2O reactions on 3.2 wt % Ru/Al_2O_3 reduced at 873 K (44.2% Ru dispersion) (5 mg of catalyst, 873 K, total flow rate 100 cm^3/min 20 kPa CO_2 or H_2O in (a) and 10 kPa CH_4 in (b), balance He).

TABLE 2: Forward CH_4 Reaction Rate, Rate Constants, and Kinetic Isotope Effects for CH_4 Reforming Reactions on 3.2 wt % Ru/Al_2O_3 Reduced at 873 K (44.2% metal dispersion) (873 K, 25 kPa CH_4 or CD_4, 25 KPa CO_2 or H_2O, balance Ar, total flow rate 100 cm^3/min)

co-reactant	turnover rate (s^{-1})[a]	rate constant (s^{-1} kPa^{-1})	kinetic isotope effect[b]	activation energy (kJ/mol)	Pre-Exponential Factor (s^{-1} kPa^{-1})	
					measured	estimated[c]
CO_2	3.9	0.16	1.42	96	8.7×10^4	5.5×10^3
H_2O	4.2	0.18	1.40	91	4.7×10^4	5.5×10^3
none	3.8	0.15	1.51	99	8.4×10^4	5.5×10^3

[a] Initial CH_4 turnover rate on Ru surface. [b] k_{CH_4}/k_{CD_4}. [c] Calculated on the basis of transition-state theory treatments of CH_4 activation steps proceeding via an immobile activated complex.[32]

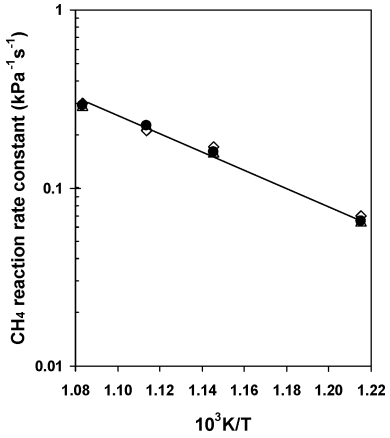

Figure 4. Arrhenius plots for CO_2 reforming (●), H_2O reforming (◇), and CH_4 decomposition (△) rate constants on 3.2 wt % Ru/Al_2O_3 reduced at 873 K (44.2% Ru dispersion).

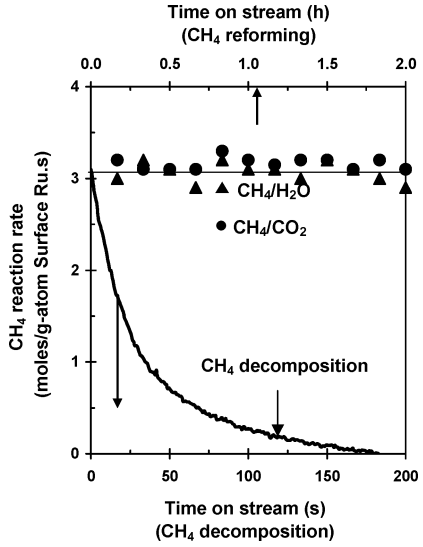

Figure 5. CH_4 reaction rate for CH_4 decomposition and reforming reactions on 3.2 wt % Ru/Al_2O_3 catalyst reduced at 873 K (44.2% Ru dispersion) (873 K, 20 kPa CH_4, 100 kPa total pressure, total flow rate 100 cm^3/min).

2. Preexponential factors predicted from transition-state theory treatments of CH_4 activation steps proceeding via immobile activated complexes[35] are also shown in Table 1. The measured values are larger than theoretical estimates, but become similar if limited mobility is assumed for activated complexes.

CH_4-CO_2 and CH_4-H_2O reaction rate constants are also similar to those measured during the early stages of CH_4 decomposition in the absence of either H_2O or CO_2 co-reactants on 3.2 wt % Ru/Al_2O_3 (Figure 5, Table 2). It appears that the sole kinetically relevant step in catalytic CH_4 reactions with H_2O or CO_2 to form H_2-CO mixtures and in stoichiometric CH_4 decomposition to form C* and H_2 on Ru is the initial activation of a C−H bond catalyzed by interactions with Ru surface atoms.

Figure 4 shows Arrhenius plots for CH_4 reforming and decomposition rate constants. Activation energies for CO_2 (96 kJ/mol), H_2O reforming (91 kJ/mol) and CH_4 decomposition (99 kJ/mol) are similar (Table 2), consistent with similar kinetically relevant steps. These activation energies resemble those reported previously for CO_2 reforming on 1.0 wt % Ru/Al_2O_3 (92.4 kJ/mol)[2] and 1.6 wt % Ru/Al_2O_3 and 4.8 wt % Ru/C (106 kJ/mol)[3], but they are much larger than reported for CH_4 activation on Ru single crystals[36,37] and on Ru/SiO_2[38] at lower temperatures. An activation energy of 51 ± 6 kJ/mol was reported for CH_4 activation on Ru (0001) from the amount of carbon deposited after various elapsed times.[36] Even lower values (36.1 kJ/mol) were measured by others on similar Ru (0001) surfaces from electron energy loss measurements of chemisorbed carbon[37] and on Ru/SiO_2 (29 kJ/mol) using a pulse microreactor.[38]

Density functional theory (DFT) led to 85 kJ/mol[39] and 78 kJ/mol[40] estimates of activation energies for CH_4 activation on Ru (0001) surfaces. These estimates lie between values measured in the present study for catalytic and stoichiometric CH_4 reaction (91−107 kJ/mol) and those reported for stoichiometric reactions on single crystals and supported clusters at lower temperatures (29−51 kJ/mol) studies. These differences remain puzzling and may well reflect the contribution of minority and catalytically irrelevant coordinatively unsaturated defects, which do not turn over because of their strong interactions with chemisorbed carbon formed in C−H activation steps. It appears, however, that rates and kinetic parameters measured during steady-state catalysis, and reflecting exclusively CH_4 activation steps, are most relevant to descriptions of catalytic surfaces at reaction conditions. It is possible that unreactive carbon deposits form at edge or kink steps in small Ru clusters and Ru single crystals; these sites would be most effective in stabilizing transition states required for C−H bond activation. If so, the resulting carbon species must be entirely unreactive during CH_4 reforming reactions, because their surface density (and consequently reaction rates) would otherwise depend on the concentration and identity of co-reactants. They must also form very rapidly during initial contact with CH_4 reactants, in view of the lack of detectable deactivation at our reaction conditions.

Differences among activation energies measured on catalysts and on model surfaces were also observed on Rh,[25] Pt,[26] Ir,[27] and Ni[28] catalysts. CO oxidation rates measured on Rh,[25] Pt,[26] and Ir[27] before and after reforming reactions were identical, indicating that the density and type of exposed metal atoms were unchanged during catalytic reforming reactions. We cannot exclude that a very small fraction of surface atoms, with remarkable reactivity in stoichiometric CH_4 activation but unable to turn over, are initially exposed on fresh samples but become unavailable during initial contact with CH_4 reactants. We conclude, however, that such sites, if present, do not turn over;

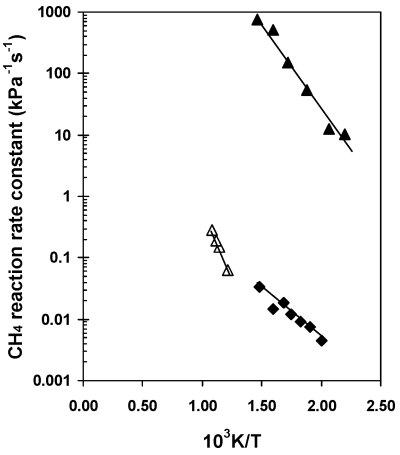

Figure 6. Arrhenius plots for CH_4 decomposition rate constants on 3.2 wt % Ru/Al_2O_3 (this study) (△), 2.75 wt % Ru/SiO_2[38] (◆), and Ru (0001)[36] (▲).

thus, they are not relevant to the analysis and prediction of catalytic rates of CH_4-H_2O and CH_4-CO_2 reactions. Indeed, Wang et al.[41] examined CH_4 decomposition on stepped Pd (679) surfaces and showed that C* preferentially forms at steps and kinks, while (111) terraces remain largely uncovered. On Pt surfaces, carbon also forms preferentially at step sites during *n*-hexane reactions, while terrace sites remain uncovered and active for catalytic reactions.[42] It is not certain that these findings are relevant to Ru surfaces and to the steady-state behavior of catalytic Ru clusters.

Figure 6 shows Arrhenius plots for CH_4 decomposition data on 3.2 wt % Ru/Al_2O_3, from the present study, together with CH_4 decomposition rates on Ru (0001)[36] and 2.75 wt % Ru/SiO_2[38] at lower temperatures. Measured CH_4 decomposition rates on Ru (0001)[36] are ~100 times larger than on Ru/Al_2O_3, while CH_4 decomposition rates are similar on 3.2 wt % Ru/Al_2O_3 and 2.75 wt % Ru/SiO_2.[38] Thus, it appears that the type of defect sites responsible for CH_4 activation on large single crystals are not available on small Ru metal clusters, even though surfaces of small clusters are often described as quite rough and densely populated by coordinatively unsaturated sites. One possibility is that this description becomes inappropriate at high temperatures, because of the tendency of small metal clusters to melt, at least in near-surface regions, well below the melting temperature of the corresponding bulk metal.[43,44] This process leads to a liquidlike layer a few atoms thick stabilized by a crystalline metal core, which becomes apparent above 800 K for Pt clusters about 8 nm in diameter, even though bulk Pt melts at 2042 K.[43,44] Smaller clusters and the presence of a support to stabilize molten structures would favor these phenomena and lead to significant loss of coordinative unsaturation for the supported Ru clusters of this study (bulk Ru melts at 2607 K). Thus, catalytic reactions at high temperatures, such as CH_4 reforming, on small metal clusters may be unable to benefit from coordinative unsaturation, even when such unsaturated sites were able to undergo a catalytic turnover. Although this explanation remains speculative at this point, it deserves additional examination in view of its marked consequences on the choice of models systems that describe faithfully the relevant features of small clusters of catalytic relevance.

Mechanistic Evidence from Kinetic Isotope Effects. Several steady-state isotopic tracer studies and kinetic isotope effect (KIE) measurements were used to probe the role and reversibility of specific elementary steps involved in CH_4-H_2O and CH_4-CO_2, as well as the mechanistic relevance of co-reactants on supported Ru catalysts. Kinetic isotope effects were measured from the relative forward rates of CH_4-CO_2 and CD_4-CO_2 reactant mixtures at 873 K on 3.2 wt % Ru/Al_2O_3 (reduced at 873 K; 44.2% dispersion). Kinetic isotope effects for H_2O reforming reactions were obtained from forward reaction rates with CH_4-H_2O, CD_4-H_2O, or CD_4-D_2O reactant mixtures also at 873 K.

Normal kinetic isotopic effects were measured for both CH_4-CO_2 and CH_4-H_2O reactions and for CH_4 decomposition (Table 2), and their values were identical within experimental accuracy (1.40−1.51). These similar values are consistent with equivalent kinetically relevant C−H bond activation steps in all three reactions. Forward reaction rates were identical for CD_4-H_2O and CD_4-D_2O reactant mixtures, indicating that activation of co-reactants and any reactions between adsorbed species formed from co-reactants and CH_4 do not influence overall reaction rates.

Elmasides and Verykios[45] measured a kinetic isotope value of 1.6 for partial oxidation of CH_4-O_2 reactant mixtures at 903 K on Ru/TiO_2. This value is very similar to those reported here for H_2O and CO_2 reforming reactions, suggesting that partial oxidation, probably occurring via sequential combustion and reforming reactions, may also be limited by C−H bond activation. Kinetic isotope effects for H_2O reforming, CO_2 reforming, or CH_4 decomposition reactions on Ru have not been previously reported. The values reported here are similar to those reported previously for CH_4 decomposition on Ni/SiO_2 (1.60) at 773 K[46] and for CO_2 reforming on Ni/Al_2O_3 (1.45) at 873 K,[47] as well as to those we recently have reported on Rh (1.54-1.60),[25] Pt (1.58−1.77),[26] Ir (1.68−1.75),[27] and Ni (1.62−1.71).[28] Another study,[48] however, failed to detect a kinetic isotope effect for CO_2 reforming on Ni at near-equilibrium conversions, which led to the proposal that H_2O or CO_2 co-reactant activation and chemisorbed oxygen atoms were involved in rate-determining steps. These latter data are inconsistent with the kinetically relevant step and the kinetic isotope effects reported here on Ru-based catalysts; they appear to reflect thermodynamic instead of kinetic isotope effects, because these measurements were made at CH_4 conversions near thermodynamic equilibrium.

Bradford and Vannice[2] proposed that CH_4-CO_2 reactions proceed on Ru surfaces via reversible CH_4 dissociation to form adsorbed CH_x and H species, followed by quasi-equilibrated steps, in which CO_2 adsorbs, dissociates, reacts with CH_x and hydroxyl groups to form CH_xO species and H. In this proposal, CH_xO ultimately dissociates to form adsorbed CO and H, which then desorb to form CO and H_2. This mechanism provides plausible elementary steps for CO_2-CH_4 reactions, but introduces a level of detail that cannot be experimentally tested, because these steps become kinetically irrelevant and the corresponding reactive intermediates are spectroscopically inaccessible when their concentrations are low during steady-state catalysis, as inferred from our kinetic and isotopic studies. We propose instead a set of elementary steps involving simpler intermediates, including chemisorbed carbon, because of its likely formation reactions that lead sequentially from CH_4 to C* with increasing rate as H-atoms are sequentially abstracted from CH_4.[49]

These elementary steps are shown as Scheme 1. CH_4 decomposes to C* in a series of elementary H-abstraction steps, with the first abstraction as the kinetically relevant step because of the low prevalent concentration of all CH_x* intermediates. This step is followed by the removal of the fragments formed using CO_2 or H_2O co-reactants.

SCHEME 1: Sequence of Elementary Steps for CH_4 Reforming Reactions on Ru-Based Catalysts

$$CH_4 + 2* \xrightarrow{k_1} CH_3* + H* \quad (8)$$

$$CH_3* + * \longrightarrow CH_2* + H* \quad (9)$$

$$CH_2* + * \longrightarrow CH* + H* \quad (10)$$

$$CH* + * \longrightarrow C* + H* \quad (11)$$

$$CO_2 + 2* \overset{K_2}{\rightleftharpoons} CO* + O* \quad (12)$$

$$C* + O* \underset{k_{-3}}{\overset{k_3}{\rightleftharpoons}} CO* + * \quad (13)$$

$$CO* \overset{K_4}{\rightleftharpoons} CO + * \quad (14)$$

$$H* + H* \rightleftharpoons H_2* + * \quad (15)$$

$$H_2* \rightleftharpoons H_2 + * \quad (16)$$

$$H* + O* \rightleftharpoons OH* + * \quad (17)$$

$$OH* + H* \rightleftharpoons H_2O* + * \quad (18)$$

$$H_2O* \rightleftharpoons H_2O + * \quad (19)$$

In this scheme, $\rightarrow$ denotes an irreversible step, and $\rightleftharpoons$ a quasi-equilibrated step, and k_i is the rate coefficient and K_i the equilibrium constant for step i. CH_4 irreversibly decomposes in a sequence of elementary steps to form chemisorbed carbon and hydrogen atoms. When (*) is the most abundant surface intermediate, only the rate constant for step (8) appears in the rate expression and the rate becomes proportional to CH_4 and independent of the presence or concentration of CO_2 or H_2O co-reactants. Steps (12), and (14)−(19) are assumed to be reversible and quasi-equilibrated. We note that these elementary steps provide pathways for reactions of CH_4 with either CO_2 or H_2O and also for water-gas shift reactions, which have been frequently, but inappropriately and nonrigorously, treated as a separate independent kinetic process in many previous studies of CH_4 reforming reactions.

Isotopic Tracer and Exchange Evidence for the Reversibility of Specific Elementary Steps. The reversibility of some of the elementary steps shown in Scheme 1 was probed using isotopic tracer and exchange methods. The reversibility of CH_4 activation steps was determined from measurements of the rate of formation of CH_xD_{4-x} ($0 < x < 4$) isotopomers during chemical conversion of $CH_4/CD_4/CO_2$ mixtures. A $CH_4/CD_4/CO_2$ (1:1:2) mixture was allowed to react at 873 K on 3.2 wt % Ru/Al_2O_3 (treated at 873 K; 44.2% dispersion). Chemical conversion and isotopic scrambling rates were measured using on-line mass spectrometry after removing $H_xD_{2-x}O$ in a trap held at 218 K (to avoid interference between fragments for H_2O, HDO, and D_2O and for CH_xD_{4-x}). The rates of CH_xD_{4-x} ($0 < x < 4$) formation and of methane chemical conversion are shown in Figure 7. The CH_4/CD_4 cross-exchange turnover rate, defined as the sum of the rates of formation of CHD_3, CH_2D_2 (taken twice), and CH_3D, is 0.18 s^{-1}. The turnover rate for CH_4 chemical conversion (3.3 s^{-1}) was about 19 times greater than for isotopic cross-exchange. The approach to equilibrium for this reaction, η, estimated from the prevalent concentrations of all reactants and products is 0.04, corresponding to the ratio of the forward overall reaction rate to the reverse reaction rate of 25, indicating that formation of traces of CHD_3, CH_2D_2, and CH_3D isotopomers is merely due to some slight reversibility for the overall reaction, which rigorously requires that the rate-determining step become exactly as reversible as the overall reaction. C−H bond activation steps on Ru crystallites at 873 K are irreversible, except as required by the approach of the overall reaction to thermodynamic equilibrium.

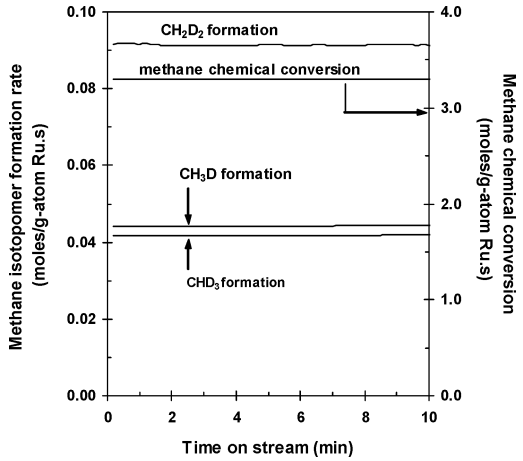

Figure 7. Methane reaction rate and CH_4/CD_4 cross-exchange rates during the reaction of $CH_4/CD_4/CO_2$ mixture on 3.2 wt % Ru/Al_2O_3 catalyst (5 mg of catalyst, 873 K, 12.5 kPa CH_4 and CD_4, 25 kPa CO_2, balance Ar, total flow rate 80 cm^3/min).

The H/D ratio in the dihydrogen formed from equimolar CH_4-CD_4 mixtures was greater than one (1.50), and dihydrogen molecules show a binomial isotopomer distribution. This H/D ratio reflects the higher reactivity of CH_4 relative to CD_4, as shown from independent reaction rates for these two methane isotopomers (1.42). The binomial distribution of dihydrogen isotopomers indicates that recombinative hydrogen desorption steps are quasi-equilibrated during CH_4-CO_2 reactions on Ru at 873 K.

Reactions of $CH_4/CO_2/D_2$ (1:1:0.2) mixtures at 873 K on 3.2 wt % Ru/Al_2O_3 were used to probe the reversibility of elementary steps leading to the formation of water and dihydrogen. Here, water was not removed before mass spectrometric analysis, and all transfer lines were kept above 373 K to prevent water condensation. No deuterated methane isotopomers were detected, as expected from the irreversible nature of C−H bond activation steps; as a result, water isotopomer measurements were unaffected by mass fragments from deuterated methane molecules. The H/D fraction expected if all H-atoms in the converted CH_4 molecules and all D-atoms in the inlet D_2 stream contributed to surface intermediates is 0.76. The water molecules formed during reaction and the dihydrogen molecules in the effluent stream both contained identical H/D ratios of 0.74. Thus, dihydrogen and water molecules and their corresponding precursors in the chemisorbed phase are in quasi-equilibrium. Table 3 shows the isotopomer distribution in water molecules formed from $CH_4/CO_2/D_2$ reactant mixtures. The isotopomer distribution is binomial with a D-content identical to that in the available reactant pool; this is consistent with fast and quasi-equilibrated recombination of H* and OH* in step (18) in Scheme 1. Binomial distributions were also observed for dihydrogen isotopomers, as expected from reversible and quasi-equilibrated recombinative hydrogen desorption steps (step (15) and (16) in Scheme 1) during CH_4/CO_2 reactions on Ru-based catalysts. In view of the kinetic equivalence of elementary steps involved in CH_4 reactions with CO_2 and H_2O, we consider these conclusions to be also valid for CH_4-H_2O reactions on Ru-based catalysts.

The reversibility of CO_2 activation steps (step (12) in Scheme 1) was probed using $^{12}CH_4/^{12}CO_2/^{13}CO$ (1:1:0.4) reactant

TABLE 3: Distribution of Water Isotopomers during Reactions of $CH_4/CO_2/D_2$ Mixtures on 3.2 wt % Ru/Al_2O_3 Reduced at 873 K (873 K, 16.7 kPa CH_4, 16.7 kPa CO_2, 3.3 kPa D_2, balance Ar, total flow rate 150 cm^3/min)

	Distribution (%)	
isotopomer	measured (H/D = 0.74)	binomial (H/D[a] = 0.76)
H_2O	0.19	0.19
HDO	0.48	0.49
D_2O	0.33	0.32

[a] (H/D) ratio predicted from H in reacted methane and D_2 in ambient stream if complete mixing between the two isotopes occurred during reaction.

mixtures at 873 K on 3.2 wt % Ru/Al_2O_3. The ^{13}C fraction in CO (0.275) and CO_2 (0.256) molecules in the effluent are similar to each other at all reaction temperatures, even though the inlet reactant mixture contained isotopically pure $^{12}CO_2$ and ^{13}CO. The ^{13}C content corresponds to complete chemical and isotopic equilibration between CO and CO_2, even at CH_4 chemical conversion levels (6.4%) far from equilibrium ($\eta = 0.06$). These data indicate that CO_2 activation steps are much faster than kinetically relevant CH_4 dissociation steps, and that steps (12) and (14) occur in both directions many times in the time required for a CH_4 chemical conversion turnover. Thus, CO_2 activation steps are reversible and quasi-equilibrated during CH_4-CO_2 reactions and by kinetic analogy also during CH_4-H_2O reactions at similar reaction conditions. Only trace amounts of $^{13}CH_4$ were detected during reactions of $^{12}CH_4/^{12}CO_2/^{13}CO$ mixtures, as expected from the low value of η (0.06) during these experiments, which lead to essentially irreversible conversion of CH_4 to H_2 and CO.

Steps (12) and (14)−(19) in Scheme 1 describe the reverse water-gas shift reaction, which must, in view of the equilibrated nature of its component steps, also be quasi-equilibrated during CH_4 reforming reactions on Ru-based catalyst (Figure 2). Indeed, we find that the approach to equilibrium for this reaction, estimated from the prevalent concentrations of all reactants and products, is near unity at all conditions (Figure 2).

These isotopic studies were carried out on a 3.2 wt % Ru/Al_2O_3 and predominately at 873 K, but the similar rate expressions obtained at all temperatures and on all catalysts do not indicate any mechanistic shifts with changes in reaction temperature or catalyst composition and thus support the general relevance of the proposed elementary steps. We note that these elementary steps also provide a rigorous basis for kinetic treatments of carbon filament formation during CH_4 reforming reactions by defining a concentration or thermodynamic activity for chemisorbed carbon as a function of prevalent pressures and of rate constants and equilibrium constants for elementary steps, as we discuss in detail elsewhere.[25−28]

Dispersion and Support Effects on H_2O and CO_2 Reforming on Ru. Ru clusters with a range of dispersion were prepared by varying the metal content, the reduction temperature, and the identity of the support. Turnover rates were calculated from forward rates normalized by the number of exposed Ru atoms; they are shown for CH_4-CO_2, CH_4-H_2O, and CH_4 decomposition reactions in Table 1. CH_4-CO_2 turnover rates reported by Bradford and Vannice,[2] Ferreria-Aparicio et al.,[12] Portugal et al.,[18] and Solymosi et al.[3] on Ru-based catalysts are also shown in Table 1. We have corrected these literature rates for approach to equilibrium and extrapolated to our reaction conditions (873 K, 20 kPa CH_4) using a first-order CH_4 dependence and the activation energies reported in each literature report (92.5 kJ/mol, Solymosi et al.[3]; 106 kJ/mol, Bradford et al.[2]). Portugal et al.[18] and Ferreria-Aparicio et al.[12] did not report activation energies; therefore, we have used our value of the activation energy (96 kJ/mol) in extrapolating their data to our reaction conditions. Forward CH_4 reaction rates were reported by Bradford et al.[2] and Portugal et al.,[18] but the net rates reported by Solymosi et al.[3] and Ferreria-Aparicio et al.[12] were converted to forward rates, using η values of 0.05 and 0.1, respectively, based on their respective CH_4 conversion levels.

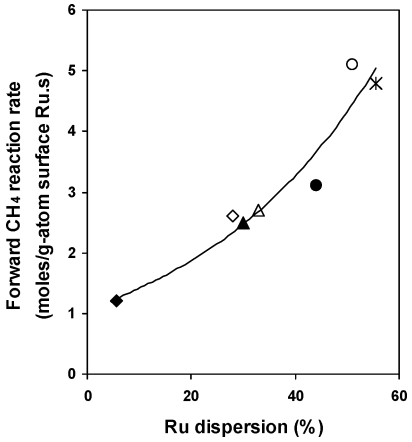

Figure 8. Forward CH_4 reaction rate for CO_2 reforming of CH_4 vs metal dispersion on different Ru-based catalysts (873 K, 20 kPa CH_4, (◆)1.0 wt % Ru/γ-Al_2O_3 (ref 3), (C) 1.0 wt % Ru/NaY (ref 18), (△)3.2 wt % Ru/ZrO_2 (this study), (●) 3.2 wt % Ru/γ-Al_2O_3 reduced at 1023 K (this study), (○) 1.6, 3.2 wt % Ru/γ-Al_2O_3 reduced at 873 K, (*) 0.64 wt % Ru/γ-Al_2O_3 (ref (12)).

Identical dispersion effects and turnover rate values were obtained for CH_4-H_2O, CH_4-CO_2, and CH_4 decomposition reaction rates (Table 1), as expected from their rigorous mechanistic equivalence. Turnover rates increased monotonically with increasing Ru dispersion for both reactions, suggesting that coordinatively unsaturated Ru surface atoms, likely to be prevalent in small crystallites even if they become mobile at high temperatures, are more active than those in low-index planes predominately exposed on large Ru crystallites. Edge and corner atoms, with fewer Ru neighbors than those on terraces, bind CH_x and H more strongly and apparently decrease the energy required to form the relevant transition state for C−H bond activation.[36] No previous literature reported systematic Ru dispersion effects on CH_4 reaction rates, but similar effects of coordinative unsaturation were previously reported on other metal surfaces.[24−28,50,51]. Klier et al.[24] found that CH_4 dissociation rates on a Pd single crystal increased with increasing density of steps and kinks. These coordinative unsaturated surface atoms showed reaction rates 10−100 times larger than on hexagonal closed-packed Pd(111) surfaces. Johnson and Weinberg[50] reported that defects sites on Ir surfaces were much more active than terrace sites for alkane dissociation reactions. Molecular beam studies by Weaver et al.[51] showed that surface defects in Pt(111) markedly increased alkane dissociation rates.

The identity of the support did not directly influence turnover rates (Table 1, Figure 8), but it can influence Ru dispersion and, in this manner, also turnover rates. Matsui et al.[9] have reported much higher CH_4 conversions on Ru/Y_2O_3 and Ru/ZrO_2 (25−29%) than on Ru/SiO_2 (12%) and attributed these effects to CO_2 activation on the supports, but neither Ru dispersions nor turnover rates were reported. These support effects are inconsistent with our findings on Al_2O_3 and ZrO_2 supports and with the kinetic irrelevance of co-reactant activation during CH_4 reforming reactions on Ru-based catalysts.

Figure 8 shows that literature turnover rates show a consistent effect of dispersion, irrespective of the identity of the support, except for the data Bradford et al.[2] on Ru/η-Al_2O_3, which showed higher turnover rates and Ru/C, which showed lower turnover rate. Once Ru dispersions are used to normalize reaction rates, turnover rates increased monotonically with increasing Ru dispersion. These dispersion effects, and the measured turnover rates, are identical for CH_4 reactions with either H_2O or CO_2 co-reactants and also for CH_4 decomposition on supported Ru catalysts (Table 1).

Conclusions

Isotopic studies and forward reaction rate measurements led to a simple mechanistic picture and to a unifying kinetic treatment of CH_4-CO_2, CH_4-H_2O, and CH_4 decomposition reactions and of water-gas shift on Ru-based catalysts. CH_4 reactions are limited by C−H bond activation and unaffected by the identity or concentration of co-reactants or of the presence of reaction products. Turnover rates were identical for CH_4 decomposition, CO_2 reforming, and H_2O reforming reactions, and activation energies were similar for the latter two reactions. The kinetic relevance of C−H bond activation was confirmed by kinetic isotope effect measurements; isotope effects were identical for CH_4-CO_2 and CH_4-H_2O reactions and for CH_4 decomposition. Cross-exchange rates are much smaller than chemical conversion rates for $CH_4/CD_4/CO_2$ mixtures and indicate that C−H bond activation is exactly as reversible as the overall chemical reaction. Reactions of the $CH_4/CO_2/D_2$ mixture led to binomial isotopomer distributions of water and dihydrogen and to D-contents identical to those expected from quasi-equilibrated water and dihydrogen desorption steps. $^{12}CH_4/^{12}CO_2/^{13}CO$ mixtures led to identical ^{13}C contents in CO and CO_2, consistent with equilibrated CO_2 dissociation steps. These results demand that the water-gas shift reaction be at thermodynamic equilibrium during CO_2 and H_2O reforming reactions on Ru-based catalysts, as indeed found from the chemical composition of the reactor effluent at all reaction conditions.

Forward turnover rates for both CO_2 and H_2O reforming increased monotonically with increasing Ru dispersion, suggesting that the coordinatively unsaturated surface atoms prevalent in small crystallites are significantly more active than those in the low-index planes predominately exposed on large crystallites. No effects of supports, beyond their influence on Ru dispersion, were detected, as expected from the kinetic irrelevance of co-reactant activation steps, which have been previously and nonrigorously claimed to occur on support sites.

Acknowledgment. This study was supported by BP as part of the Methane Conversion Cooperative Research Program at the University of California at Berkeley. Helpful technical discussions with Drs. John Collins and Theo Fleisch (BP) are gratefully acknowledged.

Appendix

The effects of the catalyst pellet size and the extent of dilution within the catalyst particles were studied on 3.2 wt % Ru/Al_2O_3 (reduced at 873 K, Ru dispersion 44.2%) for H_2O/CH_4 reactions at 873 K. The results are shown in Figure 9. Varying the diameter of catalyst pellets (250−425 vs 63−106 μm) or the extent of dilution within the pellets (5:1 to 10:1) did not influence net CH_4 reaction rates, indicating that measured net rates are not affected in any way by intrapellet or interpellet transport artifacts. Extrapolating the net reaction rate to zero residence time gives forward CH_4 reaction rates.

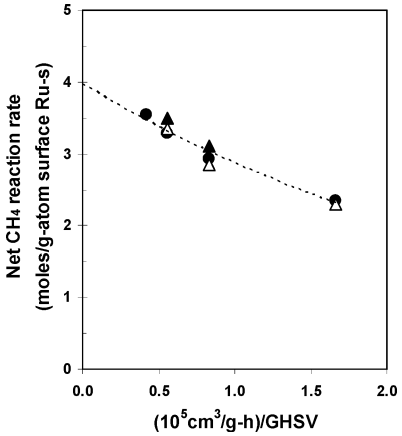

Figure 9. Net CH_4 turnover rates versus residence time for CH_4-H_2O reaction on 3.2 wt % Ru/Al_2O_3 at 873 K((●) 10 mg of catalyst diluted with 100 mg of Al_2O_3 within pellets, then diluted with 500 mg of ground quartz, pellet size 250−425 μm; (Δ) 10 mg of catalyst diluted with 50 mg of Al_2O_3 within pellets, then diluted with 500 mg of ground quartz, pellet size 250−425 μm; (▲) 10 mg of catalyst diluted with 50 mg of Al_2O_3 within pellets, then diluted with 500 mg of ground quartz, pellet size 63−106 μm).

References and Notes

(1) Fischer, V. F.; Tropsch, H. *Brennstoff-Chemie* **1928**, *3*, 39.
(2) Bradford, M. C. J.; Vannice, M. A. *J. Catal.* **1999**, *183*, 69.
(3) Solymosi, F.; Kustan, G.; Erohelyi, A. *Catal. Lett.* **1991**, *11*, 149.
(4) Claridge, J. B.; Green, M. L. H.; Tsing S. C. *Catal. Today* **1994**, *12*, 455.
(5) Vernon, P. D. F.; Green, M. L. H.; Cheetham, A. K.; Ashcroft, A. T. *Catal. Today* **1992**, *13*, 417.
(6) Ashcroft, A. T.; Cheetham, A. K.; Green, M. L. H.; Vernon, P. D. F. *Nature* **1991**, *352*, 225.
(7) Basini, L.; Sanfilippo, D. *J. Catal.* **1995**, *157*, 162.
(8) Matsui, N.; Nakagawa, K.; Ikenaga, N.; Suzuki, T. *J. Catal.* **2000**, *194*, 115.
(9) Matsui, N.; Anzai, K.; Akamatsu, N.; Nakagawa, K.; Ikenaga, N.; Suzuki, T. *Appl. Catal. A: General* **1999**, *179*, 247.
(10) Mark, F. M.; Maier, W. F. *J. Catal.* **1996**, *164*, 122.
(11) Ferreira-Aparicio, P.; Rodriguez-Ramos, I.; Anderson, J. A.; Guerrero-Ruiz, A. *Appl. Catal. A* **2000**, *202*, 183.
(12) Ferreira-Aparicio, P.; Marquez-Alvarez, C.; Rodriguez-Ramos, I.; Schuurman, Y.; Guerrero-Ruiz, A.; Mirodatos, C. *J. Catal.* **1999**, *184*, 202.
(13) Sutton, D.; Parle, S. M.; Ross, J. R. H. *Fuel Process. Technol.* **2002**, *75*, 45.
(14) Bradford, M. C. J.; Vannice, M. A. *Catal. Today* **1999**, *50*, 87.
(15) Qin, D.; Lapszewicz, J. *Catal. Today* **1994**, *21*, 551.
(16) Rostrup-Nielsen, J. R.; Hansen, J. H. B. *J. Catal.* **1993**, *144*, 38.
(17) Guerrero-Ruiz, A.; Ferreira-Aparicio, P.; Bachiller-Baeza, M. B.; Rodriguez-Ramos, I. *Catal. Today* **1998**, *46*, 99.
(18) Portugal, U. L.; Marques, C. M. P.; Araujo, E. C. C.; Morales, E. V.; Giotto, M. V.; Bueno, J. M. C. *Appl. Catal. A* **2000**, *193*, 173.
(19) Schuurman, Y.; Mirodatos, C.; Ferreira-Aparicio, P.; Rodriguez-Ramos, I.; Guerrero-Ruiz, A. *Catal. Lett.* **2000**, *66*, 33.
(20) Pitchai, R.; Klier, K. *Catal. Rev.-Sci. Eng.* **1986**, *28*, 13.
(21) Boudart, M. *Adv. Catal.* **1969**, *20*, 153.
(22) McMaster, M. C.; Madix, R. J. *J. Chem. Phys.* **1993**, *98*, 15.
(23) Gee, A. T.; Hayden, B. E.; Mormiche, C.; Kleyn, A. W.; Riedmuller, B. *J. Chem. Phys.* **2003**, *118*, 3334.
(24) Klier, K.; Hess, J. S.; Herman, R. G. *J. Chem. Phys.* **1997**, *107*, 4033.
(25) Wei, J.; Iglesia, E. *J. Catal.*, in press.
(26) Wei, J.; Iglesia, E., *J. Phys. Chem. B* **2004**, *108*, 4094.
(27) Wei, J.; Iglesia, E. Angew *Chem. Int. Ed.*, in press.
(28) Wei, J.; Iglesia, E., *J. Catal.*, in press.
(29) Bahlawane, N.; Watanabe, T. *J. Am. Ceram. Soc.* **2000**, *83*, 2324.
(30) Barton, D. G. Ph.D. dissertation, University of California at Berkeley, 1998.
(31) Mazzieri, V.; Coloma-Pascual, F.; Arcoya, A.; Largentière, P. C.; Fígoli, N. S. *Appl. Surf. Sci.* **2003**, *210*, 222.
(32) Price, G. L.; Iglesia, E. *Ind. Eng. Chem.* **1989**, *28*, 839.

(33) Stull, D. R.; Edgar, F.; Westrum, J.; Sinke, G. C. *The Thermodynamics of Organic Compounds*; Robert, E., Ed.; Krieger Publishing Co.: Malabar, FL, 1987.
(34) Boudart, M.; Djega-Mariadassou, G. *The Kinetics of Heterogeneous Catalytic Reactions*; Princeton University Press: Princeton, NJ, 1984.
(35) Dumesic, J. A.; Rudd, D. F.; Rekoske, J. E.; Trevino, A. A. *The Microkinetics of Heterogeneous Catalysis*; American Chemical Society: Washington, DC, 1993.
(36) Egeberg, R. C.; Ullmann, S.; Alstrup, I.; Mullins, C. B.; Chorkendorff, I. *Surf. Sci*. **2002**, *497*, 183.
(37) Wu, M. C.; Goodman, D. W. *Surf. Sci.* **1994**, *306*, L529.
(38) Carstens, J. N.; Bell, A. T. *J. Catal*. **1996**, *161*, 423.
(39) Ciobica, I. M.; Frechard, F.; van Santen, R. A.; Kleyn, A. W.; Hafner, J. *J. Phys. Chem. B* **2000**, *104*, 3364.
(40) Liu, J. P.; Hu, P. *J. Am. Chem. Soc.* **2003**, *125*, 1958.
(41) Wang, Y.; Herman, R. G.; Klier, K. *Surf. Sci*. **1992**, *279*, 33.
(42) Davis, S. M.; Zaera, F.; Somorjai, G. A. *J. Catal*. **1982**, *77*, 439.
(43) Wang, Z. L.; Ahmad, T. S.; El-Sayed, M. A. *Surf. Sci.* **1997**, *380*, 302.
(44) Wang, Z. L.; Petroski, J. M.; Green, T. C.; El-Sayed, M. A. *J. Phys. Chem. B* **1998**, *102*, 6145.
(45) Elmasides, C.; Verykios, X. E. *J. Catal*. **2001**, *203*, 477.
(46) Otsuka, K.; Kobayashi, S.; Takenaka, S. *J. Catal*. **2001**, *200*, 4.
(47) Osaki, T.; Horiuchi, T.; Suzuki, K.; Mori, T. *Catal. Lett.* **1997**, *44*, 19.
(48) Schuurman, Y.; Kroll, V. C. H.; Ferreira-Aparicio, P.; Mirodatos, C. *Catal. Today* **1997**, *38*, 129.
(49) Au, C.; Ng, C.; Liao, M. *J. Catal*. **1999**, *185*, 12.
(50) Johnson, D. F.; Weinberg, W. H. *J. Chem. Phys.* **1994**, *101*, 6289.
(51) Weaver, J. F.; Krzyzowski, M. A.; Madix, R. J. *Surf. Sci.* **1997**, *391*, 150.